7th International Conference on Multiphase Flow,
ICMF 2010, Tampa, FL, May 30 – June 4, 2010

Phenomenological Heat Transfer Model of Micro Two-Phase Slug Flow without Phase Change

Y. Hasegawa, N. Kasagi and A. Yamamoto

Department of Mechanical Engineering, The University of Tokyo, Hongo 7-3-1, Bunkyo-ku, Tokyo 113-8656, Japan

Keywords: micro two-phase flow, heat transfer, modelling

Abstract

We investigate the heat transfer and pressure loss characteristics of gas-liquid slug flow in a micro tube. Experimental results suggest that injection of slight amount of gas into liquid flow enhances heat transfer with favorable pressure penalty. As a result, the heat transfer per unit pumping power becomes larger than that in the single-phase laminar flow. Numerical results clearly show that a circulation generated in the liquid slug plays an important role in enhancing the heat transfer. In order to predict the effect of different flow patterns on the heat transfer, we model the overall heat transfer as one-dimensional unsteady heat conduction inside the liquid film with a time-dependent heat transfer rate between the film and the slug regions. It is found that the present model predicts the overall heat transfer rate fairly well under a wide rage of flow patterns

Nomenclature

Roman symbols

C_p	thermal capacity, [J/kg K]
D	tube diameter, [m]
h	heat transfer coefficient, [W/K m^2]
j	superficial velocity, [m/s]
L	longitudinal length, [m]
Nu	Nusselt number
p	pressure, [Pa]
Pe	thermal Peclet number,$\rho_L U C_{pL} D/\lambda_L$
Pr	Prandtl number
q	heat flux, [W/m^2]
r	radial direction, [m]
R	tube radius, [m]
Re	Reynolds number, $\rho_L U D/\eta_L$
t	time, [s]
T	temperature, [K]
$\vec{u}$	velocity
We	Weber number, $\rho_L U^2 D/\sigma$
z	longitudinal direction, [m]

Greek symbols

α	thermal diffusion coefficient [m^2/s]
β	volumetric flow ratio
δ	residual film thickness, [m]
ϵ	void fraction
σ	surface tension coefficient, [N/m]
μ	viscosity, [Pa s]
ν	kinematic viscosity, [m^2/s]
λ	thermal conductivity, [W/m K]
ψ	dimensionless stream function
ρ	density,[kg/m^3]

Subscripts

g	gas phase
l	liquid phase
TP	two-phase

Introduction

Gas-liquid two-phase flow without phase change is a possible way of heat transfer enhancement for compact heat exchangers. The presence of gas bubbles separating discrete liquid slugs causes a circulation inside the liquid phase so that the overall heat transfer is enhanced. Moreover, such gas-liquid flows are rather stable due to absence of explosive boiling. These facts open up a possibility of achieving better heat transfer with moderate pressure penalty. The structure and behavior of such tow-phase flow, however, are inherently complex, so that basic understanding the flow and heat transfer mechanisms is essential.

A number of experimental visualizations have been carried out in order to clarify the flow characteristics of adiabatic gas-liquid two-phase flow in micro tubes (Tripletter et al. 1999; Kawahara et al., 2002; Serizawa et al., 2002.). Recently, it has been shown that the flow pattern in a micro tube is not uniquely determined with the flow rates of gas and liquid, but strongly depends on the inlet condition. Once a flow pattern is reached down-

stream of the inlet, it remains unchanged even far downstream (Hayashi et al., 2007; Kawaji et al., 2009). These facts suggest a possibility to control the flow pattern so as to achieve favorable heat transfer characteristics by modifying the inlet condition. However, there exist few studies conduct simultaneous measurement of the heat transfer and pressure loss characteristics in these flows.

One of the most fundamental problems is to predict the heat transfer rate based on the flow parameters, such as the slug lengths and flow rates of gas and liquid. A typical phenomenological model is the three-zone flow boiling model proposed by Thome et al. (2003). Although this model has been successfully applied to boiling and condensation in a micro tube, there exists no model applicable to gas-liquid slug flow without phase change.

In the present work, the pressure loss and heat transfer characteristics of gas-liquid two phase flow without phase change in a micro tube are measured. In order to study the detailed mechanisms of heat transfer, we also carry out a series of numerical simulations. Base on the numerical results, we decompose the whole flow field into an adherent liquid film near the wall and the gas-liquid slug regions. It is shown that the transient temperature fluctuation inside the liquid film is a key to predict the overall heat transfer rate. We analyze a one-dimensional transient heat conduction problem inside the liquid film, and then develop a heat transfer model as a function of parameters representing the flow pattern. Finally, we verify the present model through comparison with the numerical results.

Experimental Measurement

Experimental Setup. The schematic figure of the present experimental setup is shown in Fig. 1. Water is used as a continuous phase, while gaseous nitrogen as a dispersed phase. The liquid flow rate and the gas flow rate are controlled by a twin plunge pump (GL sciences, PU714) and a mass flow controller (Yamatake Co., CMQ-V 5 ml/min), respectively. In order to visualize flow patterns, a micro glass tube with the inner and outer diameter of 500 and 800 μm is used in the test section. The gas and liquid phases are mixed through coaxial tubes at the inlet as shown in Fig. 2. A fine stainless steel tube is inserted into the micro glass tube. The inner and outer diameter of the inner tube are 300 and 400 μm, respectively. Nitrogen is introduced from the inner pipe, while water from the outer annular section. Table 1 shows the experimental conditions. In the present study, the gas superficial velocity j_g is systematically changed from 0.02 to 0.3 m/s while the liquid superficial velocity j_l is kept constant. Throughout this manuscript, the subscripts of l and g represent values in the liquid and

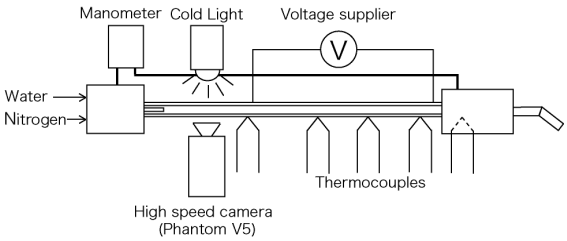

Figure 1: Experimental Setup.

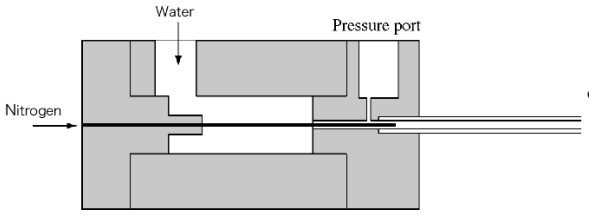

Figure 2: Inlet Condition.

gas phases, respectively. Two different j_l, i.e., $j_l = 0.06$ and 0.2 m/s are considered. It was confirmed that the flow patterns in the above conditions are periodic gas-liquid slug flows, and the gas and liquid slug lengths are kept constant in each case. Under these conditions, we measure the gas and liquid slug lengths, heat transfer rate and pressure loss.

A mixture of ITO and silver is uniformly sputtered on the outer surface of the glass tube for the heating element. This enable us to visualize the flow pattern with a high-speed camera (Vision Research, Phantom v5). Each image has 1024 x 128 pixels and the frame rate was 1000$\sim$4000 frames/sec. From visualization images, we estimate the gas and liquid slug lengths. The outer wall temperature $T_{wall_{out}}$ is measured with K-type thermocouples, calibrated with the accuracy of 0.1 K. By solving one-dimensional steady heat conduction problem inside the tube wall, we estimate the inner wall temperature $T_{wall_{in}}$ From the heat flux q and $T_{wall_{in}}$, the two-phase heat transfer rate is obtained as follows:

$$h_{TP} = \frac{q}{T_{wall_{in}} - T_{bulk}} \tag{1}$$

We also measure the pressure at the inlet and the outlet in order to obtain the pressure loss within the test section. The inlet pressure loss is estimated in a single-phase flow experiment and this value is subtracted from the obtained pressure loss in the two-phase flow experiments.

Results. In Fig. 3, the heat transfer rate, the pressure loss and the heat transfer per unit pumping power are shown when j_g is systematically increased while j_l is kept constant. The horizontal axis represents the void

Table 1: Experimental Conditions.

Inner Path	Outer Path	Liquid Superficial Velocity [m/s]	Gaseous Superficial Velocity [m/s]	Heat Flux [kW/m^2]
Water	Nitrogen	0.06, 0.2	0.02∼0.3	27∼62

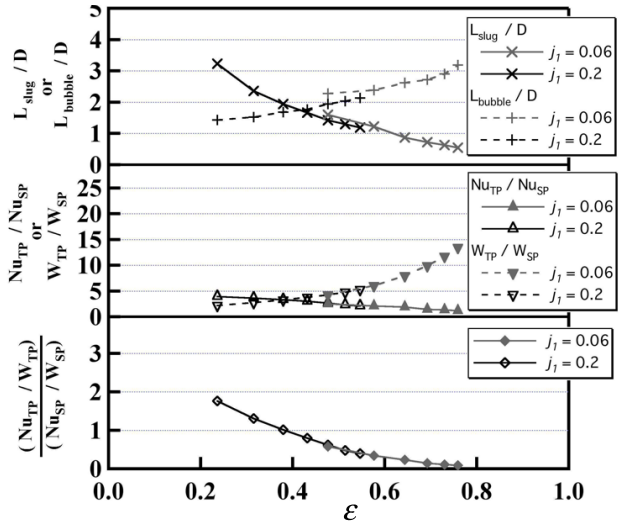

Figure 3: Performances of gas-liquid two phase flow

fraction $\epsilon = j_g/(j_g + j_l)$, while the heat transfer rate, the pressure loss and the heat transfer per unit pumping power are all normalized by the quantities of the single phase flow, i.e., $\epsilon = 0$.

It is found that with increasing ϵ, the liquid slug length monotonically decreases, while the gas slug length increases. In addition, the effect of j_l is minor so that the flow pattern is mainly determined by ϵ. In accordance with the change of the flow pattern, the heat transfer rate also monotonically decreases with increasing ϵ, while the pressure loss increases drastically. Consequently, the heat transfer per unit pumping power monotonically decreases with ϵ. We note that the heat transfer per unit pumping power becomes larger than that in a single phase flow when the void fraction is small, i.e., $0 < \epsilon < 0.3$. This suggests that the heat transfer characteristics is improved from those in a single phase flow by introducing small amount of gas in the liquid flow.

Numerical Simulation

Numerical Method. In order to study the effects of a flow pattern on the heat transfer characteristics, we conduct numerical simulations of a gas-liquid two-phase flow with heat transfer in a cylindrical pipe. It is assumed that each phase is incompressible and phase change does not take place. The temperature is considered as a passive scalar. The gravity is neglected due to dominance of the surface tension. The interface is captured by using the Phase-Field method (Anderson et al., 1998). The dimensionless governing equations are given as follows:

$$\nabla \cdot \vec{u} = 0, \tag{2}$$

$$\frac{\partial(\rho\vec{u})}{\partial t} + \vec{u}\cdot\nabla(\rho\vec{u}) = -\nabla p + \frac{1}{Re_{TP}}\nabla\cdot[\eta(\nabla\vec{u} + \nabla\vec{u}^T)] - \frac{\gamma C\nabla f}{Cn\cdot We}, \tag{3}$$

$$\frac{\partial(\rho C_p T)}{\partial t} + \vec{u}\cdot\nabla(\rho C_p T) = \frac{1}{Pe_l}\nabla\cdot\lambda\nabla T, \tag{4}$$

where, ρ, μ, C_p and λ denote the density, viscosity, thermal capacity and conductivity, respectively, and all these quantities are normalized by the values of liquid.

The dimensionless parameters appear in Eqs. (3-4) are defined as:

$$Re_{TP} = \frac{\rho_l^* U_{TP}^* D^*}{\mu_l^*}, \quad We = \frac{\rho^* U_{TP}^{*2} D^*}{\sigma^*},$$
$$Pe_l = Re_{TP} Pr_l = \frac{\rho_l^* C_{pl}^* U_{TP}^* D^*}{\lambda_l^*}, Pr_l = \frac{\nu_l^*}{\alpha_l^*}, \tag{5}$$

where a value with an asterisk denotes a dimensional quantity, while D^* is the tube diameter. The thermal diffusion coefficient is denoted by $\alpha^* = \lambda^*/\rho^* C_p^*$. The characteristic velocity U_{TP}^* is defined as the sum of superficial liquid and gas velocities, i.e., $U_{TP}^* = j_g^* + j_l^*$.

Equations of (2) - (4) are satisfied both in gas and liquid phases, and the local fluid properties of ρ, μ, λ and C_p are interpolated between those of gas and liquid according to the position of interface.

The flow is assumed to be periodic with constant gas and liquid slug lengths. Therefore, only one period of the flow is simulated with a pair of gas and liquid slugs. In addition, the flow is assumed axisymmetric, so that a two-dimensional $(r - z)$ computational domain is employed. The periodic length $L_z = L_z^*/R^*$ defines the computation domain, where R^* is the tube radius. In the present study, L_z is changed as $3 \le L_z \le 15$ with different gas and liquid slug lengths. A periodic boundary condition is applied at the two ends of the computational domain, while the no-slip and fully wetted boundary conditions are used on the tube wall. For the temperature field, a uniform heat flux q is assumed along the wall. Because only the temperature difference is of interest, a quasi-periodic boundary condition, namely,

$$\left.\frac{\partial T}{\partial z}\right|_{z=0} = \left.\frac{\partial T}{\partial z}\right|_{z=L_z}, \tag{6}$$

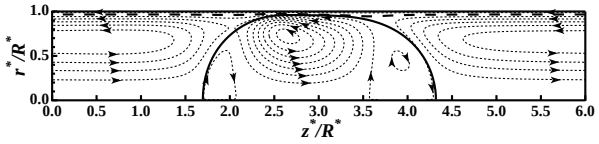

Figure 4: Bubble shape and relative streamlines at $\epsilon = 0.29$ and $Re_{TP} = 288$. thick solid line: gas-liquid interface, thick broken line: dividing streamline between an adherent liquid film and gas-liquid slugs

is applied on the both ends of the computation domain.

In accordance with the present experiment conditions, water and Nitrogen at 293 K and 1 atm are assumed as working fluids, and the surface tension σ^* is 0.0728 N/m. The tube diameter D^* is fixed at 600μm, and the characteristic velocity U^*_{TP} is given as 0.03$\sim$1.5m/s. This range covers both bubbly and slug flows according to experimental observation (Hayashi et al., 2007). The Prandtl number in liquid is $Pr_l = 6.96$.

Results. The contours of the dimensionless stream function ψ relative to the bubble motion in a typical case, where $L_z = 6.0$ and the void fraction $\epsilon = 0.29$ are shown in Fig. 4. Here, ψ is defined as:

$$\frac{1}{r}\frac{\partial \psi}{\partial r} = u_z - U_{bubb}, \quad \frac{1}{r}\frac{\partial \psi}{\partial z} = -u_r, \tag{7}$$

where U_{bubb} is the velocity of the moving bubble. As illustrated in Fig. 4, a large anti-clockwise circulation is found inside the gas phase between smaller clockwise circulations in the front and rear of a gas bubble. The circulation can also be found in the liquid region. The present result agrees with the sketch by Taylor (1961) and the visualization by Thulasidas et al. (1997).

Comparison between the Nusselt numbers obtained by simulation and experiment under the same flow rates and slug lengths of gas and liquid is shown in Fig. 5. Although qualitative agreement is confirmed, quantitative agreement between the simulation and the experiment is not obtained in the present study. This can be mainly attributed to a measurement error in the experiment. Especially, when the heat transfer rate is high, the difference between the inner-wall temperature and the bulk temperature becomes quite small so that high accuracy in the temperature measurement is required. This remains as future work.

Heat Transfer Modelling

Basic Concept. The present heat transfer model is schematically shown in Figs. 6 a, b). The whole domain is modelled as an adherent liquid film with alternatively

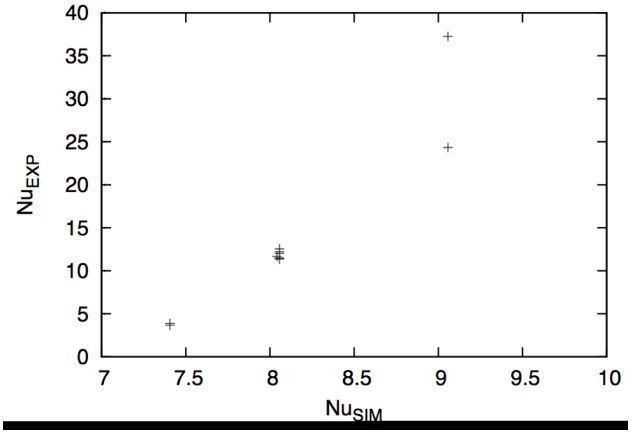

Figure 5: Comparison between the Nusselt numbers obtained by simulation and experiment

passing gas and liquid slugs (see, Fig. 6 a)). The adherent film spans beneath both the gas and liquid slugs. For simplicity, both gas and liquid slugs are modelled as cylinders with radius of $R_{slug} = R - \delta$. We assume that the liquid film is stagnant and its thickness δ is constant along the wall. We have confirmed that these assumptions are reasonable for all flow conditions considered here. Due to the no-slip condition at the wall, we assume that the velocity inside the adherent film is negligible so that all gas and liquid injected into the micro tube is assumed to flow in the slug region, which is now defined as, $r < R_{slug}$. Therefore, the ratio of the gas and liquid slug lengths, i.e., L_{bubble} and L_{slug} is given by:

$$\frac{L_{bubble}}{L_{slug}} = \frac{\beta_g}{\beta_l}, \tag{8}$$

where β_l and β_g denote the volumetric flow fractions of liquid and gas, respectively. Obviously, $\beta_l + \beta_g = 1$, $0 \le \beta_l \le 1$ and $0 \le \beta_g \le 1$.

Since the heat capacity and conductivity of gas are negligible, while the liquid film thickness is sufficiently small, we model the overall heat transfer as a one-dimensional unsteady heat conduction inside the liquid film with a time-dependent heat transfer rate at the interface between the film and slug regions as illustrated in Fig. 6 b).

Formulation Since $\delta \ll R$, we neglect the effect of the tube curvature inside the liquid film and the distance from the wall is denoted by y hereafter. This transient one-dimensional heat conduction problem in the y direction can be described as:

$$\frac{\partial T^*}{\partial t^*} = \alpha^* \frac{\partial^2 T^*}{\partial y^{*2}}. \tag{9}$$

Here, T^* and α^* are the temperature and the thermal diffusion coefficient in liquid. At the bottom wall, a con-

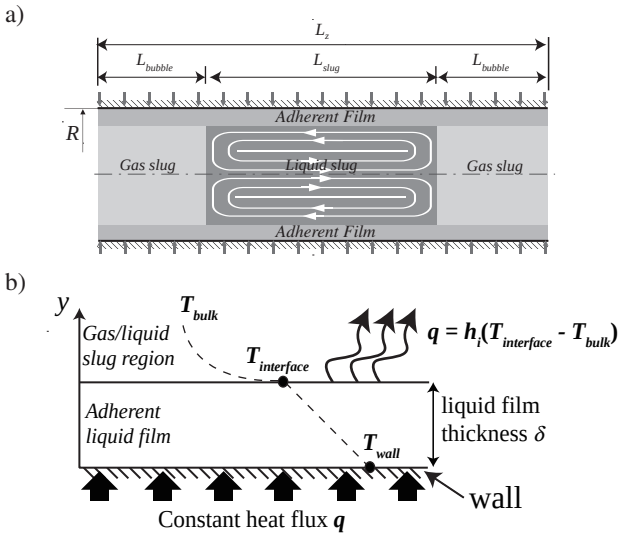

Figure 6: Conceptual figures of the present heat transfer model a) Decomposition of the entire flow field; b) Heat transfer modelling inside the adherent liquid film.

stant heat flux condition is applied:

$$-\lambda^* \frac{\partial T^*}{\partial y^*} = q^* = const. \;\; at \;\; y^* = 0. \tag{10}$$

At the interface between the slug and film regions, a thermal boundary condition of the third kind is assumed:

$$-\lambda^* \frac{\partial T^*}{\partial y^*} = h_i^*(t) T^* \;\; at \;\; y^* = \delta^*. \tag{11}$$

Note that we shift the temperature so that the bulk temperature is zero so that T^* represents the temperature deviation form the bulk temperature. Here, h_i is the interfacial heat transfer rate from the liquid film to the slug region.

Considering that the heat capacity and conductivity of the gas phase are quite small, h_i should be negligible when a gas bubbule passes above the liquid film. In addition, assuming that the heat transfer rate h_{slug} of the liquid slug is uniform along the streamwise direction, $h_i(t)$ can be modelled as:

$$\begin{aligned} h_i^*(t) &= h_{slug}^*, \;\; 0 < t^* < t_l^*, \\ h_i^*(t) &= 0, \;\; t_l^* < t^* < t_p^*. \end{aligned} \tag{12}$$

Here, t_p^* is the entire period, while t_l^* is the duration in which the liquid slug passes above the liquid film. Hence, $t_p^* = t_l^* + t_g^*$, where t_g^* is the gas slug passage duration. In the slug region, we assume that the gas and liquid slugs travel at the same velocity. Therefore, t_l^* and t_g^* are given by L_{slug}^*/U_{TP}^* and L_{bubble}^*/U_{TP}^*, respectively. Now, the major task is to find how the total heat transfer rate h_{TP}^* from the bottom wall to the bulk fluid should be correlated with h_{slug}^*, t_l^*, t_g^* and δ^*.

Dimensionless parameters The energy equation (9) are normalized as follows:

$$\frac{\partial T}{\partial t} = Fo \frac{\partial^2 T}{\partial y^2}, \tag{13}$$

where the temperature T, time t and distance from the bottom wall y are normalized by $\Delta T^* = q^* \delta^* / \lambda^*$, t_p^* and δ^*, respectively. The Fourier number is defined as $Fo = \alpha^* t_p^* / \delta^{*2}$.

Similarly, the boundary conditions of Eqs. (10) and (11) are respectively normalized as:

$$\frac{\partial T}{\partial y} = -1 \;\; at \;\; y = 0, \tag{14}$$

$$\frac{\partial T}{\partial y} = -B_i h_i(t) T \;\; at \;\; y = 1. \tag{15}$$

Here, B_i is the Biot number defined as $B_i = \overline{h_i} \delta^* / \lambda^*$ and h_i is normalized by its mean value as $h_i = h_i^* / \overline{h_i^*}$ so that:

$$\begin{aligned} h_i(t) &= \beta_l^{-1}, \;\; 0 < t < \beta_l, \\ h_i(t) &= 0, \;\; \beta_l < t < 1. \end{aligned} \tag{16}$$

Here, t_l^*/t_p^* is replaced with β_l, since we assume that the gas and liquid flow in the slug region is homogeneous.

From the above, the heat transfer rate is governed by the three dimensionless parameters, i.e., Bi, Fo and β_l.

Two-Layer Heat Conduction Model. It was observed that the temperature fluctuation mainly occurs in the near-interface region, i.e., $1 - \eta_t \leq y \leq 1$, while the temperature is almost steady in the outer region, i.e., $0 \leq y \leq 1 - \eta_t$. Here, the thermal penetration thickness η_t can be estimated by the liquid-slug passage time β_l and the dimensionless conductivity Fo as $\eta_t = \alpha \sqrt{Fo \beta_l}$, where $\alpha \sim 0.55$.

In view of the above result, we further divide the liquid film into two layers. In the first layer adjacent to the interface, the temperature temporally fluctuates in response to h_i. In the second layer, the temperature is assumed to be steady. Eventually, the Nusselt number Nu_{f_model} predicted in the present model is given by:

$$\begin{aligned} Nu_{f\_model} &= \frac{1}{\overline{T}(0)} \\ &= \left[\frac{1 - \beta_g^2}{B_i} + \frac{Fo \beta_g^2}{\eta_t} \left\{ \frac{1}{1 - \exp(-\frac{B_i Fo}{\eta_t})} - \frac{1}{2} \right\} + 1 \right]^{-1} \end{aligned} \tag{17}$$

For detailed derivation of the above equation, please refer to He et al. (2010). The comparison between the

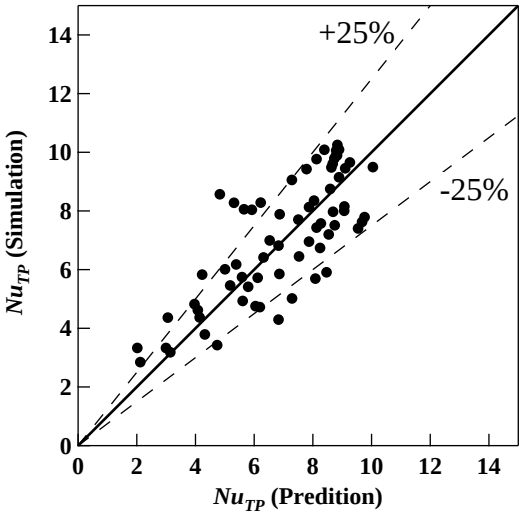

Figure 7: Comparison between the numerical simulation and the model prediction

model predictions and the numerical results is shown in Fig. 7. The Nusselt number obtained in the present simulation varies from 2.85 to 10.25 depending on the flow pattern. It is confirmed that the present model predict the numerical data fairly well under a wide rage of flow patterns.

Conclusions

We investigate heat transfer and pressure loss characteristics in micro gas-liquid two phase flow. It was found that injection of small amount of gas into liquid flow enhances heat transfer with less increase of pressure penalty. As a result, the heat transfer per unit pumping power is enhanced in the two phase flow compared to the single phase flow. In order to study the mechanisms of heat transfer, we also conducted a series of numerical simulations. It was found that the Nusselt number strongly depends on the flow pattern, and is upt to 2.4 times higher than that of the single-phase laminar flow.

The streamline function in the entire flow domain shows that the gas-liquid slug flow is generally characterized by an adherent liquid film with alternate passage of gas and liquid slugs above the film. In order to predict the effects of the flow pattern on the heat transfer, we model the overall heat transfer as one-dimensional unsteady heat conduction inside the liquid film with a time-dependent heat transfer rate between the film and slug regions.

The present model is useful in optimizing the flow pattern so as to achieve the highest heat transfer performance with the minimum pressure penalty. The optimization of the flow pattern remains as future work.

Acknowledgements

The authors are grateful to Dr. Q. He for providing his valuable numerical data.

References

Anderson, D.M., McFadden, G.B. and Wheeler, A.A., Diffuse-interface methods in fluids mechanics, Annu. Rev. Fluid Mech., Vol. 30, pp.139-165, 1998

Hayashi, S., Kasagi, N. and Suzuki, Y., The effects of inlet flow conditions on gas-liquid two-phase flow in a micro tube, Proc. HT2007 & 2007 ASME-JSME Thermal Engineering Summer Heat Transfer Conference, Paper No. HT2007-32916, Vancouver, July 8-12, 2007

He, Q., Hasegawa, Y. and Kasagi, N., Heat transfer modelling of gas-liquid slug flow without phase change in a micro tube Int. J. Heat Fluid Flow, Vol. 31, pp.126-136, 2010

Kawaji, M., Mori, K. and Bolintineanu, The effects of inlet geometry and gas-liquid mixing on two-phase flow in microchannels, ASME J. Fluids Engineering, Vol. 131, 041302 1-7, 2009

Kawahara, A., Chung, P.M.-Y and Kawaji, M., Investigation of two-phase flow pattern, void fraction and pressure drop in a microchannel, Int. J. Multiphase Flow, 28, pp.1411-1435, 2002

Serizawa, A., Feng, Z. and Kawara, Z., Two-phase flow in microchannels, Experimental Thermal and Fluid Science, Vol. 26, 703–714, 2002.

Thome, J.R., Hajal, J.E. and Cavallini, A., Condensation inhorizontal tubes, Part 2: New heat transfer model based on flow regimes, Int. J. Heat Mass Transfer, Vol. 46, pp. 3365-3387, 2003

Triplett, K.A., Ghiaasiann, S.M., Abdel-Khalik, S.I. and Sadowski, D.L., Gas-liquid two-phase flow in microchannels. Part I: two-phase flow patterns, Int J. Multiphase Flow, Vol. 24, pp.377-394, 1999.

Thulasidas, T.C., Abraham, M.A. and Cerro, R.L., Flow patterns in liquid slugs during bubble-train flow inside capillaries, Chem. Eng. Sci., Vol. 52, pp.2947-2962, 1997